HHS Public Access

Author manuscript

Oncogene. Author manuscript; available in PMC 2017 January 14.

Published in final edited form as:

Oncogene. 2016 July 14; 35(28): 3636–3646. doi:10.1038/onc.2015.429.

E2f3 in tumor macrophages promotes lung metastasis

Prashant Trikha[1,2,3], **Nidhi Sharma**[1,2,3], **Clarissa Pena**[1,2,3], **Andreas Reyes**[1,2,3], **Thierry Pécot**[1,2,3], **Safiya Khurshid**[1,2,3], **Maysoon Rawahneh**[1,2,3], **Julie Moffitt**[1,2,3], **Julie A. Stephens**[4], **Soledad A. Fernandez**[4], **Michael Ostrowski**[5], and **Gustavo Leone**[1,2,3,*]

[1]Human Cancer Genetics Program, The Ohio State University, Columbus, Ohio 43210, USA.

[2]Department of Molecular Virology, Immunology and Medical Genetics, College of Medicine and Public Health, The Ohio State University, Columbus, Ohio 43210, USA.

[3]Department of Molecular genetics, College of Biological Sciences, The Ohio State University, Columbus, Ohio 43210, USA.

[4]Center for Biostatistics, College of Medicine, The Ohio State University, Columbus, Ohio 43210, USA.

[5]Department of Molecular Cellular Biochemistry, College of Medicine and Public Health; The Ohio State University, Columbus, Ohio 43210, USA.

Abstract

The Rb-E2F axis is an important pathway involved in cell cycle control that is deregulated in a number of cancers. E2f transcription factors have distinct roles in the control of cell proliferation, cell survival and differentiation in a variety of tissues. We have previously shown that E2fs are important downstream targets of a CSF-1 signaling cascade involved in myeloid development. In cancer, tumor associated macrophages (TAMs) are recruited to the tumor stroma in response to cytokines secreted by tumor cells and are believed to facilitate tumor cell invasion and metastasis. Using the *MMTV-Polyoma Middle T antigen* (*PyMT*) mouse model of human ductal carcinoma, we show that the specific ablation of *E2f3* in TAMs, but not in tumor epithelial cells, attenuates lung metastasis without affecting primary tumor growth. Histological analysis and gene expression profiling suggests that *E2f3* does not impact the proliferation or survival of TAMs, but rather controls a novel gene expression signature associated with cytoskeleton rearrangements, cell migration and adhesion. This *E2f3*-TAM gene expression signature was sufficient to predict cancer recurrence and overall survival of ER-positive breast cancer patients. Interestingly, we find that *E2f3b* but not *E2f3a* levels are elevated in TAMs from *PyMT* mammary glands relative to controls, suggesting a differential role for these isoforms in metastasis. In summary, these findings identify *E2f3* as a key transcription factor in TAMs that influences the tumor microenvironment and tumor cell metastasis.

[*]Corresponding Author Information: Human Cancer Genetics Program, Department of Molecular Virology, Immunology and Medical Genetics, The Ohio State University, Comprehensive Cancer Center, 460 W. 12th Ave., Columbus, OH 43210, Telephone: 614-688-4567, FAX: 614-292-3312, Gustavo.Leone@osumc.edu.

Conflict of Interest: “The authors disclose no potential conflicts of interest.”

Keywords

E2fs; metastasis; stroma; macrophages and breast cancer

Introduction

Breast cancer is the second leading cause of cancer mortality in women with approximately 30% patients eventually developing metastasis [34]. Metastasis is a complex process during which tumor cells colonize distant organ sites [9, 11]. Metastasis contributes to 90% of deaths from solid tumors and displays diverse clinical manifestations [22]. The tumor stroma or microenvironment plays a crucial role in the dissemination of tumor cells from the primary cancer. Tumor stroma is composed of extracellular as well as cellular constituents, including fibroblasts, endothelial and immune cells. During tumor progression, the tumor stroma may be altered to influence the neoplastic properties of tumor cells and facilitate their dissemination [12, 22]. One of the extreme examples of how stromal cells can drive tumorigenesis was shown by Kim and colleagues where selective deletion of *Smad4* in T-cells resulted in formation of epithelial cancer in the gastrointestinal tract of mice [24].

The initial response of immune cells in cancer is to recognize and destroy tumor cells. However, strategies in tumor cells to escape, suppress immune destruction or convert immune cells to have pro-tumorigenic roles often evolve [15]. Tumor associated macrophages (TAMs) are recruited to the tumor stroma in response to cytokines secreted by both tumor epithelial cells and other resident stromal cells [7, 12]. In addition, TAMs also activate myofibroblasts to secrete cytokines that help in the recruitment of endothelial progenitor cells and promote neovascularization [36]. Clinical studies show that infiltration of TAMs correlates with poor prognosis in a variety of cancers [25, 41] and that therapeutic strategies to limit macrophage numbers are effective at decreasing cancer development [2]. Similarly, depletion of macrophages using pharmacological agents, such as clodronate reduces tumor angiogenesis and metastasis in various mouse models of cancer [16, 30, 32].

Colony stimulating factor 1 (CSF-1) secreted by tumor cells facilitates the recruitment of TAMs, which in turn promote the invasion and migration of tumor cells by the secretion of EGF [47]. Mice lacking the CSF-1 ligand (op/op) have reduced incidence of pulmonary metastasis [27]. In human breast cancer overexpression of CSF-1 correlates with poor prognosis and dense leukocyte infiltration [23]. The engagement of the CSF-1 receptor by CSF-1 leads to the activation of numerous signaling cascades during normal myeloid development, including the Rb/E2f pathway, which is involved in regulating cell proliferation, survival and differentiation [42].

Genetic alterations of *RB* have been reported in approximately 20-30% of breast cancers [5, 21]. RB exerts its tumor suppressive effects through the regulation of E2F transcription factors [33]. Increased E2F3 expression has been reported in prostate, ovarian and lung cancers [13, 14, 18, 35] and amplification of 6p22, which includes the *E2F3* locus, has been observed in bladder cancer [35]. Introduction of miR-148a and miR-34b/c in tumor cells target E2F3 and result in a reduction of tumor growth and metastasis [28]. Collectively, these

studies imply that *E2F3* is frequently overexpressed or amplified in a number of cancers and that its reduction may deter cancer progression.

We have previously shown that E2fs are important downstream targets in CSF-1 signaling cascade involved in macrophage development [42]. However, the role of *E2f3* in the tumor microenvironment (stroma) remains to be investigated. Here, we address the potential role of *E2f3* in TAMs during mammary tumorigenesis. To this end, we examined the consequence of ablating *E2f3* in either TAMs or tumor cells on tumor progression and lung metastasis using the *MMTV-Polyoma Middle T antigen* (*MMTV-PyMT)* mouse model of breast cancer. We show that the loss of *E2f3* in tumor macrophages, but not in mammary tumor cells, leads to the attenuation of lung metastasis without affecting the growth of the primary tumor.

Results

Loss of one copy of *E2f3* reduces lung metastasis

To investigate the role of *E2f3* during mammary gland tumorigenesis in mice, we used the *MMTV-Polyoma Middle T antigen* (*PyMT*) model of breast cancer. The advantage of this model is that there is rapid tumor progression accompanied by immune infiltration and lung metastasis. We generated *PyMT;E2f3*$^{+/+}$ (n=36) and *PyMT;E2f3*$^{+/-}$ (n=19) female mice to determine whether the loss of one *E2f3* allele would affect tumor growth and metastasis. Mice were palpated twice a week and time to tumor was recorded once the tumor volume reached 5mm^3. Kaplan Meier plots show that loss of one copy of *E2f3* had no effect on the timing of tumor onset (Figure 1A) or tumor burden (Figure 1B), suggesting that loss of a single *E2f3* allele does not affect tumor development by the *PyMT* oncogene. Moreover, histopathological analysis of tumors isolated from *PyMT;E2f3*$^{+/+}$ and *PyMT;E2f3*$^{+/-}$ mice revealed no gross pathological differences between the two groups of mice (Figure 1C). However, examination of lungs at end-stage showed a significant reduction of metastasis in *PyMT;E2f3*$^{+/-}$ mice (Figures 1D and 1E). In addition, to the lungs we also examined the bones, spleens and livers from *PyMT;E2f3*$^{+/}$-and found no signs of metastasis at these sites.

Since *E2f3* null mice are not viable, we used a conditional *E2f3* allele and a bitransgenic system where the expression of *Cre* is under the control of the mouse mammary tumor virus promoter (*MMTV-rtTa;teto-Cre*) to specifically ablate *E2f3* in the mammary ductal epithelium. Two cohorts of female mice were generated (*PyMT;E2f3*$^{loxp/loxp}$*;MMTV-rtTa* and *PyMT;E2f3*$^{loxp/loxp}$*;MMTV-rtTa;teto-Cre*) and fed with food containing doxycycline (1mg/kg). Surprisingly, ablation of *E2f3* in *PyMT;E2f3*$^{loxp/loxp}$*;MMTV-rtTa; teto-Cre* mice resulted in a slight but significant delay in tumor initiation ($p<0.003$), but had little impact on tumor burden and metastasis to the lungs (Supplementary Figure S1A-S1C). Examination of mammary glands revealed no change in tumor cell proliferation or macrophage infiltration between the two cohorts of mice (Supplementary Figure S1D). Together, these results suggest that the reduction of lung metastasis initially observed in *PyMT; E2f3*$^{+/-}$ mice may be mediated through a cell non-autonomous mechanism.

E2f3 ablation in TAMs leads to the reduction of lung metastasis

Macrophages are an important part of tumor stroma and have been shown to be important in tumor cell dissemination during metastasis [12, 22]. Given that global deletion of one allele of *E2f3* led to a decrease in lung metastasis, we entertained the hypothesis that E2f3 in macrophages may contribute to metastasis in mice. To test this hypothesis we used the *Lysozyme Cre* (*LysCre*) transgene to conditionally inactivate *E2f3* in macrophages and compare tumor growth and metastasis in *PyMT;LysCre;E2f3*$^{loxp/loxp}$, *PyMT;LysCre; E2f3*$^{+/loxp}$ and *PyMT;E2f3*$^{loxp/loxp}$ mice. PCR genotyping of macrophages isolated from tumors and lungs showed that *Cre* expression resulted in deletion of *E2f3*, albeit not in one hundred percent of cells (Figure 2A).

While the tumor burden in the three cohorts of mice was similar (Figure 2B and 2C), lung metastasis in *PyMT;LysCre; E2f3*$^{loxp/loxp}$ and *PyMT;LysCre; E2f3*$^{+/loxp}$ were significantly reduced (p<0.01) when compared to *PyMT;E2f3*$^{loxp/loxp}$ (control) mice (Figure 2D and 2E). We measured macrophage numbers by immuno-histochemistry (IHC) staining using F4/80-antibody on early adenomas (80-old day tumor mice) and late stage carcinomas (110- day old tumor mice). This analysis revealed no significant changes in macrophage numbers in tumors at either early or late stages of progression or in lung metastasis when *E2f3* was deleted in macrophages (Figures 3A-3B and S2-S3), suggesting that *E2f3* is not required for the proliferation of TAMs. Consistent with the absence of an effect on tumor burden, *E2f3* deletion in macrophages had no effect on the proliferation of tumor cells in the primary tumor or metastatic sites (Figures 3A-3B and S2). Analysis of inguinal mammary glands from virgin, pregnant and involuting *LysCre; E2f3*$^{loxp/loxp}$ and *E2f3*$^{loxp/loxp}$ mice revealed normal mammary gland development [44] (Supplementary Figure S4). Together, these results suggest that *E2f3* ablation in TAMs results in a significant reduction of lung metastasis without affecting mammary development or tumor initiation and growth.

E2f3 in lung and tumor macrophages promotes metastasis

Macrophages have been shown to contribute to tumor cell dissemination from the primary tumor or in the establishment of a metastatic niche at distant organ sites. To explore the role of *E2f3* in TAMs we first orthotopically injected highly metastatic syngeneic MVT-1 cells into the fat pad of *E2f3*$^{loxp/loxp}$ and *LysCre;E2f3*$^{loxp/loxp}$ mice and evaluated lung metastasis 4 weeks later. While tumors in both groups reached the same size, there were significantly fewer metastatic lesions in lungs of *LysCre;E2f3*$^{loxp/loxp}$ mice compared to controls (Figure 4A). F4/80 and Ki67 antibody staining of primary tumors and metastases showed no differences in either macrophage infiltration or in the proliferation of tumor cells (4B).

Next, we injected MVT-1 cells into the tail vein of *LysCre; E2f3*$^{loxp/loxp}$ and *E2f3*$^{loxp/loxp}$ mice and examined the seeding and establishment of tumor metastases in lungs. Compared to controls, deletion of *E2f3* in macrophages resulted in a significant reduction (p<0.01) of the metastatic lung area (Figure 5A). Macrophage infiltration and tumor cell proliferation at the metastatic site was similar in both groups of mice (Figure 5B). Together, these results suggest that *E2f3* in macrophages promotes the metastasis of mammary tumor cells to the lung.

Loss of *E2f3* leads to disruption of cell adhesion and cytoskeleton genes

To explore the underlying molecular mechanism by which *E2f3* in macrophages promote lung metastasis, we analyzed global gene expression in control and *E2f3* deleted TAMs using an Affymetrix platform. To this end, RNA from F4/80$^+$ TAMs collected from *PyMT; E2f3$^{loxp/loxp}$* (control) and *PyMT; LysCre; E2f3$^{loxp/loxp}$* mice was processed and used to query mouse Affymetrix 430 2.0 oligo-arrays. An unbiased method similar to Gene Set Enrichment Analysis [29] was used to identify genes that were differentially expressed between the two groups. Surprisingly, the vast majority of the 104 differentially expressed genes were upregulated in the *E2f3* deleted TAMs compared to controls (>1.5 fold, $p<0.001$; Figure 6A). Quantitative real time (RT-PCR) expression analysis confirmed the increased levels of a subset of these mRNAs in *E2f3* depleted TAMs (Figure 6B). Gene ontology of differentially expressed genes showed an enrichment of gene functions related to cell migration, adhesion, cytoskeleton and signaling networks and a conspicuous absence of cell cycle related functions (Figure 6C and Supplementary Table 1).

The matricellular proteins (*Sparcl1*, *Jam2 and Fbln5)* participate in the assembly and stabilization of extracellular matrix structures and are involved in cell adhesion and migration. Their expression has been found to be down regulated in a number of cancers [20, 38, 48]. Our microarray and RT-PCR data showed increased expression of these genes in *E2f3* deleted TAMs, suggesting that their increased expression may lead to reduced migration of tumor cells. Based on these findings, we evaluated whether deletion of *E2f3* in TAMs might impair tumor cell migration. Migration assays were performed using MVT-1 cells and conditioned media collected from TAMs of *PyMT;E2f3$^{loxp/loxp}$* (control) and *PyMT;LysCre;E2f3$^{loxp/loxp}$* mice. These assays showed a significant reduction in tumor cell migration ($p<0.0001$) when conditioned media from *E2f3* ablated TAMs was used (Figure 6D and Supplementary Figure S5A).

Sequence analysis of gene promoters revealed that 51 out of the 104 differentially expressed genes contained consensus E2F binding sites within 1kb from the transcriptional start (TS) site, and 14 of the 51 putative target promoters had E2F consensus sites that were conserved between mouse and human (Figure 6E). Analysis of a subset of these using Chromatin immunoprecipitation (ChIP) assays and F4/80$^+$ sorted TAMs from tumors showed E2f3 directly bound to these conserved gene promoters (Figure 6F and Supplementary Figure S5B).

The *E2f3* locus encodes two isoforms, *E2f3a* and *E2f3b*, whose expression is driven by distinct promoters [26]. Based on their expression pattern during the cell cycle and their ability to physically interact with Rb, it was suggested that E2f3a may function as a transcriptional activator and E2f3b as a transcriptional repressor [1]. Interestingly, RT-PCR gene expression analysis on FACS sorted F4/80$^+$ macrophages showed that *E2f3b* levels were significantly upregulated in TAMs relative to normal macrophages, whereas *E2f3a* expression was unchanged (Supplementary Figure S6). From these experiments we conclude that *E2f3b* expression in macrophages is responsive to tumor cells. While the individual roles of *E2f3a* and *E2f3b* remain to be determined, the fact that both isoforms are deleted in *PyMT;LysCre;E2f3$^{loxp/loxp}$* mice, may suggest that *E2f3b* may have a specific function in the repression of TAM related gene expression.

E2f3 TAM gene signature predicts good prognosis in breast cancer patients

To determine the relevance of these findings to human breast cancer, we used the E2F3-related TAM gene expression signature identified in Figure 6A to query previously published global expression profiles derived from laser-captured tumor stroma (49 samples) and adjacent normal stroma (52 samples) in breast cancer patients [17]. The 104-gene signature derived from mouse *E2f3* deficient TAMs was able to perfectly segregate normal from tumor stroma (Figure 7A). Many of the genes in this signature were expressed at higher levels in normal stroma when compared to tumor-stroma (Supplementary Table 2), consistent with lower levels of *E2F3* expression in the normal stroma compartment ($p<0.015$; data not shown).

To determine whether the E2F3 TAM gene signature correlated with clinical outcome, we used unsupervised clustering of expression data obtained from four independent breast cancer patient datasets. The comparison of mouse *E2f3* TAM gene signature with human breast cancer patient datasets (Finak, NKI, Stockholm and Wang) predicted a significant better overall survival ($p<0.05$) (Figure 7B). Because the NKI and Wang datasets have a large cohort of ER-positive and ER-negative breast cancer patients, we queried these two patient subsets independently. This analysis shows that the *E2f3* mouse gene signature predicted good prognosis in ER-positive, but not in ER-negative, breast cancer patients (Supplementary Figure S7). From these results we conclude that the *E2f3* TAM gene signature identified in *E2f3* deleted macrophages is represented within normal stroma and is associated with favorable clinical outcome in breast cancer patients.

Discussion

The Rb-E2F axis represents an important pathway involved in cell cycle control that is disrupted in cancer [10]. Alterations in *RB* or components that regulate the RB pathway occur in the majority of cancers, including breast cancer [5, 21]. Recent studies have demonstrated the involvement of E2Fs in driving *Her2/Neu*- and *Myc*-induced mammary tumorigenesis in mice [46]. However, the role of *E2f3* in tumor stroma during cancer progression and metastasis remains to be investigated. Using a *PyMT* mammary cancer model we show here that specific ablation of *E2f3* in TAMs attenuates lung metastasis without having a major effect on the growth of the primary tumor.

Increased *E2F3* expression has been observed in human prostate, ovarian and lung cancers [13, 18, 35]. In a mouse model of thyroid cancer, a role for *E2f3* has been implicated in the metastasis of tumor cells to the liver and lung [49], however, whether cell autonomous or non-autonomous mechanisms were at play was not determined. Using conditional knockout approaches we show that ablation of *E2f3* in TAMs results in decreased pulmonary metastasis without affecting the growth of the primary tumor, suggesting that *E2f3* in the tumor stroma has an important cell non-autonomous role in promoting the metastatic potential of tumor cells.

The E2F family of transcription factors is conserved from nematodes to mammals, with three genes encoding one activator and two repressors in *C. elegans* and eight genes encoding three activators and five repressors in humans [8]. E2Fs were identified as factors

that control the cell cycle, apoptosis, differentiation and stress responses, thus E2Fs have been bestowed with a role as master regulators of cell proliferation [33]. Studies in flies, worms and mice support a role for E2Fs beyond cell cycle control. For example, loss-of-function studies identified roles for *lin-35* (*RB1* orthologue) and *efl-1* (E2F1-3 orthologue) in epidermal growth factor mediated cell fate determination in *C. elegans* during vulval development [8]. Additional roles for mammalian E2Fs in angiogenesis, adipogenesis and cell migration have also been described [3, 8, 31].

The *E2f3* locus encodes two isoforms, *E2f3a* and *E2f3b*, whose expression is driven by distinct promoters [26]. Previous studies from the Tlsty lab show that inactivation of Rb pathway and elevated *E2f3* expression are characteristic features of basal-like cancer [19]. A recent study from our laboratory has shown increased *E2f3a* expression in tumor cells overexpressing the *Erb2/Her2* oncogene [46]. Consistent with these findings, we show here that deletion of *E2f3* in the mammary epithelium of *PyMT* mice also delays tumor onset, suggesting that the *E2f3a* isoform may have oncogenic functions, likely through promoting cell proliferation and cell survival, in a number of mammary tumor models. Whereas *E2f3a* is highly expressed in tumor cells, we observe that *E2f3b* is highly expressed in TAMs. We find that *E2f3* in TAMs directly binds to regulatory sequences of a number of genes that negatively regulate tumor cell metastasis. The expression of these genes in TAMs is increased upon the loss of the *E2f3* allele. Thus, we suggest that *E2f3b* is the likely isoform encoded by the *E2f3* locus that functions as a transcriptional repressor in TAMs to promote metastasis. Because the *Cre* mediated ablation of the *E2f3* floxed allele used here and in previous studies results in deletion of both *E2f3* isoforms, the relative contributions of each isoform during tumorigenesis remains to be rigorously determined. In the present study, we show that E2F3 controls a gene expression signature associated with cytoskeletal rearrangements and cell adhesion. Surprisingly, *E2f3* ablation in TAMs had no effect on their proliferation nor in the expression of cell cycle regulated genes. It is well recognized that the ECM is not simply a scaffold for tumor cells but instead provides critical signals that affect tumor cell growth, survival and migration [4]. For instance, one of the proteins that promote ECM deposition is secreted protein acidic and rich in cysteine (Sparc). The absence of Sparc is associated with decreased collagen deposition and $Sparc^{-/-}$ mice have enhanced tumorigenesis [4, 6].

Importantly, it was shown that Sparc produced by host leukocytes, rather than tumor cells, promotes the assembly and function of tumor-associated stroma through the organization of collagen type IV [39]. Similarly, Jam2, Fbln5 and Sparcl1 are matricellular proteins that participate in the assembly and stabilization of extracellular matrix structures involved in cell adhesion and migration. The expression of these genes is downregulated in a number of human malignancies [20, 48]. The role of these proteins in inhibiting the migration of cancer cells is well documented [4, 40]. However, the cells that produce these factors and the mechanisms involved in their gene regulation remain poorly understood. We find that ablation of *E2f3* in TAMs leads to increased expression of *Jam2, Fbln5, Col18A1, Sparcl1* and other secreted factors with roles in cell migration and adhesion, which are known to impede migration of tumor cells. Consistent with the upregulation of this secretory cell adhesion signature in *E2f3* deficient TAMs, analysis of the Finak stroma-specific dataset [17] revealed that expression of this signature was downregulated in tumor stroma relative to

normal stroma. This gene signature also predicted better survival outcomes in the Finak, NKI, Wang and Stockholm datasets [17, 37, 43, 45]. We would thus suggest that elevation of *E2f3b* expression and repression of this secretory cell adhesion signature in TAMs may play a role during tumor progression and metastasis in breast cancer patients.

Materials and Methods

Mammary Tumor Models

All animals used in the study were 5th generation FVB/N background. Mice carrying *PyMT* oncogene under control of *MMTV* promoter were used in this study. Macrophage specific deletion of $E2f3^{f/f}$ was achieved by breeding them with the mice carrying *Cre* recombinase driven by the lysozyme promoter (*LysCre*). To delete $E2f3^{loxp/loxp}$ in mammary epithelial cells, mice were bred with *MMTV–rtTA;teto-Cr*e mice. Induction of the *MMTV-rtTA/teto-Cre* system was achieved by administration of doxycycline in food (1mg/kg) at 4 weeks of age and continued until animals were sacrificed. Mice were palpated twice a week for tumors, they were considered tumor free until the tumors were 5mm. Mice were sacrificed when they were 110- days old or reached early removal criteria (ERC). Genotyping was performed on genomic DNA isolated from tail clips of the mice.

Orthotropic Injections

Briefly 2×10^5 MVT-1 cells were injected either through the tail vein or subcutaneously into the fat pad of 8-10 week old $E2f3^{loxp/loxp}$ and $LysCre;\ E2f3^{loxp/loxp}$ mice. Mice were sacrificed 2-4 weeks after the injection.

Histology and Immunohistochemistry

For whole mount staining of mammary glands, inguinal gland #4 or #9 were removed, fixed in Carnoys fixative at 4°C overnight, re-hydrated and stained with Carmine Red. Tumors and lungs removed from the mice were fixed in 10% buffered formalin and embedded in paraffin. To quantify metastatic foci in the lungs, each lobe was sectioned and stained with hemotoxylin and eosin (H&E). Image J software was used to quantify the metastatic area in each lobe of the lung. For H&E and IHC staining, 5um sections were cut, deparaffinized in xylene and rehydrated with graded ethanol series. The tumor and lung sections were then stained with either α-F4/80 **(**Invitrogen MF-48004) or α-Ki67 (Pharmingen 550609) antibodies as described below. All primary and secondary antibodies were diluted in DAKO diluent (DAKO). Sections were blocked with M.O.M. blocking reagent (Vector Labs) for 30min and incubated with primary antibody for 30min. The sections were rinsed and incubated with a biotinylated secondary antibody for 15min. Following the biotinylated secondary antibody, the streptavidin-Alexa dye conjugate was applied for 15min. Sections were washed for 5min with Phosphate-buffered saline (PBS) before incubating with DAB for 2min. Sections were washed in water and counter stained using Meyers hematoxylin followed by a brief rinse in DI water and mounted using Gel/Mount (Biomed, Foster City, CA).

Image Analysis

Images of histological and IHC sections were taken with Axio digital camera (Zeiss) mounted on the Axioskop microscope (Zeiss). Whole mount images were taken with a Coolpix 5700 digital camera (Nikon). Image files were processed using AxioVision 4.3 software (Zeiss).

Flow Cytometry

Tumors harvested from the mice were minced and digested with collagenase. Single cell suspensions were prepared after passing through a 40 micron mesh and stained with fluorochrome conjugated F4/80 antibody (Invitrogen, MF48020). After staining the cells were sorted using FACS Aria (Becton Dickinson, BD).

Microarray analysis

F4/80$^+$ TAMs were isolated from tumor samples by FACS as described above. Four independent samples from each genetic group were used for analysis by Affymetrix microarray. RNA was isolated using TRIzol reagent. RNA was then subjected to purification and processed for hybridization to Affymetrix Mouse Genome 430 2.0 Arrays. Expression values were normalized and log transformed using RMAExpress, normalized data was then analyzed using BRB-ArrayTools 3.7.0. Differentially expressed genes that increased or decreased at $p<0.001$ in *PyMT;LysCre;E2f3*$^{loxp/loxp}$ samples relative to control samples were used to generate the heatmaps. The microarray data were deposited with Gene Expression Omnibus (GEO) and can be viewed at http://www.ncbi.nlm.nih.gov/geo/ GSE67081.

Real-Time RT-PCR

RNA was isolated using Trizol reagent from F4/80$^+$ TAM. Reverse transcription of total RNA was performed using Superscript III reverse transcriptase (Invitrogen) and RNAse Inhibitor (Roche) according to the manufacturer's protocol. Real-time PCR was performed using a BioRad iCycler and reactions were performed in triplicate and relative amounts of cDNA were normalized to RPL4.

Migration Assay

TAMs were isolated from mammary tumors of *PyMT;E2f3*$^{loxp/loxp}$ (control) and *PyMT;LysCre;E2f3*$^{loxp/loxp}$ mice as described above. After FACS sorting TAMs were plated in 6 well plates in serum free media overnight following which the conditioned media was collected and used for the migration assay. Transwell inserts containing 1×10^5 MTV-1 cells were placed in 24-well plates containing conditioned media obtained from TAMs. The migration of MVT-1 cells was allowed to proceed overnight. The inserts were stained using the standard protocol following manufactures instructions. Images were acquired using Nikon microscope and number of cells were quantified using image J software.

ChIP Assays

For ChIP assays, F4/80$^+$ TAMs were crosslinked and chromatin was sonicated to an average size of 200-1000 bp. Lysates were subsequently pre-cleared with Salmon Sperm DNA/ Protein G agarose slurry. Antibodies specific to α-E2F3 (2ug, SC-878) were then added to

each sample and incubated overnight at 4°C. Antibody-protein-DNA complexes were recovered by addition of Salmon Sperm DNA/Protein G agarose slurry after incubation for 1h at 4°C. Following extensive washing, the complexes were eluted and decrosslinked at 65°C for 4h. Finally, samples were treated with Proteinase K (Roche), RNase A (Roche) and purified through Qiaquick columns (Qiagen). Real-time PCR quantification of immunoprecipitated DNA was performed using the Biorad iCycler with primers specific for the indicated promoter regions. Sequences for the primers used are available upon request.

Human Stroma Heatmap

Analysis of the mouse *E2f3* TAM microarray data led to the identification of 104 differentially expressed unique genes. These genes were queried against a published human breast stroma microarray dataset (GSE4823, henceforth referred as Finak dataset), which is publicly available and accessible through the NCBI GEO website. A heat map was generated using these genes on the Finak human stroma dataset (52 normal stroma and 49 tumor stroma samples) using hierarchical clustering with Euclidean distance measures.

Survival analyses of breast cancer patient cohorts

A Cox proportional hazards model is applied to predict an outcome for each patient from the gene expression of the human orthologs that correspond to differentially regulated genes from mouse *E2f3* TAMs. The patients are then split into two groups (high-risk and low-risk patients) and displayed in a Kaplan-Meier plot. A log-rank test was applied to evaluate statistical significance between the two groups. Details are provided in the supplementary methods.

Statistical Analyses

Data are expressed as mean ± SD. Statistical significance was determined using ANOVA and Wilcoxon Rank Sum tests.

Supplementary Material

Refer to Web version on PubMed Central for supplementary material.

Acknowledgement

We thank Bryan Mcelwain for technical assistance with flow cytometry. This work was funded by NIH grants R01CA121275, R01CA098956 and P01CA097189 to GL. P.T and N.S are recipients of the T32 fellowship (CA 106196-06).

References

1. Adams M, Sears R, Nuckolls F, Leone G, Nevins J. Complex transcriptional regulatory mechanisms control expression of the E2F3 locus. Mol Cell Biol. 2000; 20:3633–3639. [PubMed: 10779353]
2. Allavena P, Sica A, Solinas G, Porta C, Mantovani A. The inflammatory micro-environment in tumor progression: the role of tumor-associated macrophages. Crit Rev Oncol Hematol. 2008; 66:1–9. [PubMed: 17913510]
3. Blanchet E, Annicotte JS, Lagarrigue S, Aguilar V, Clapé C, Chavey C, et al. E2F transcription factor-1 regulates oxidative metabolism. Nat Cell Biol. 2011; 13:1146–1152. [PubMed: 21841792]

4. Bornstein P, Sage EH. Matricellular proteins: extracellular modulators of cell function. Curr Opin Cell Biol. 2002; 14:608–616. [PubMed: 12231357]
5. Bosco EE, Knudsen ES. RB in breast cancer: at the crossroads of tumorigenesis and treatment. Cell Cycle. 2007; 6:667–671. [PubMed: 17361100]
6. Brekken RA, Puolakkainen P, Graves DC, Workman G, Lubkin SR, Sage EH. Enhanced growth of tumors in SPARC null mice is associated with changes in the ECM. J Clin Invest. 2003; 111:487–495. [PubMed: 12588887]
7. Bronisz A, Godlewski J, Wallace JA, Merchant AS, Nowicki MO, Mathsyaraja H, et al. Reprogramming of the tumour microenvironment by stromal PTEN-regulated miR-320. Nat Cell Biol. 2012; 14:159–167. [PubMed: 22179046]
8. Ceol CJ, Horvitz HR. dpl-1 DP and efl-1 E2F act with lin-35 Rb to antagonize Ras signaling in C. elegans vulval development. Mol Cell. 2001; 7:461–473. [PubMed: 11463372]
9. Chaffer CL, Weinberg RA. A perspective on cancer cell metastasis. Science. 2011; 331:1559–1564. [PubMed: 21436443]
10. Chen H, Tsai S, Leone G. Emerging roles of E2Fs in cancer: an exit from cell cycle control. Nat Rev Cancer. 2009; 9:785–797. [PubMed: 19851314]
11. Chiang A, Massagué J. Molecular basis of metastasis. N Engl J Med. 2008; 359:2814–2823. [PubMed: 19109576]
12. Condeelis J, Pollard J. Macrophages: obligate partners for tumor cell migration, invasion, and metastasis. Cell. 2006; 124:263–266. [PubMed: 16439202]
13. Cooper C, Nicholson A, Foster C, Dodson A, Edwards S, Fletcher A, et al. Nuclear overexpression of the E2F3 transcription factor in human lung cancer. Lung Cancer. 2006; 54:155–162. [PubMed: 16938365]
14. De Meyer T, Bijsmans IT, Van de Vijver KK, Bekaert S, Oosting J, Van Criekinge W, et al. E2Fs mediate a fundamental cell-cycle deregulation in high-grade serous ovarian carcinomas. J Pathol. 2009; 217:14–20. [PubMed: 18991331]
15. DeNardo DG, Johansson M, Coussens LM. Immune cells as mediators of solid tumor metastasis. Cancer Metastasis Rev. 2008; 27:11–18. [PubMed: 18066650]
16. Diel I, Solomayer E, Bastert G. Bisphosphonates and the prevention of metastasis: first evidences from preclinical and clinical studies. Cancer. 2000; 88:3080–3088. [PubMed: 10898355]
17. Finak G, Bertos N, Pepin F, Sadekova S, Souleimanova M, Zhao H, et al. Stromal gene expression predicts clinical outcome in breast cancer. Nat Med. 2008; 14:518–527. [PubMed: 18438415]
18. Foster C, Falconer A, Dodson A, Norman A, Dennis N, Fletcher A, et al. Transcription factor E2F3 overexpressed in prostate cancer independently predicts clinical outcome. Oncogene. 2004; 23:5871–5879. [PubMed: 15184867]
19. Gauthier ML, Berman HK, Miller C, Kozakeiwicz K, Chew K, Moore D, et al. Abrogated response to cellular stress identifies DCIS associated with subsequent tumor events and defines basal-like breast tumors. Cancer Cell. 2007; 12:479–491. [PubMed: 17996651]
20. Hurley PJ, Marchionni L, Simons BW, Ross AE, Peskoe SB, Miller RM, et al. Secreted protein, acidic and rich in cysteine-like 1 (SPARCL1) is down regulated in aggressive prostate cancers and is prognostic for poor clinical outcome. Proc Natl Acad Sci U S A. 2012; 109:14977–14982. [PubMed: 22927397]
21. Jiang Z, Deng T, Jones R, Li H, Herschkowitz JI, Liu JC, et al. Rb deletion in mouse mammary progenitors induces luminal-B or basal-like/EMT tumor subtypes depending on p53 status. J Clin Invest. 2010; 120:3296–3309. [PubMed: 20679727]
22. Joyce J, Pollard J. Microenvironmental regulation of metastasis. Nat Rev Cancer. 2009; 9:239–252. [PubMed: 19279573]
23. Kacinski B. CSF-1 and its receptor in ovarian, endometrial and breast cancer. Ann Med. 1995; 27:79–85. [PubMed: 7742005]
24. Kim BG, Li C, Qiao W, Mamura M, Kasprzak B, Kasperczak B, et al. Smad4 signalling in T cells is required for suppression of gastrointestinal cancer. Nature. 2006; 441:1015–1019. [PubMed: 16791201]

25. Leek R, Lewis C, Whitehouse R, Greenall M, Clarke J, Harris A. Association of macrophage infiltration with angiogenesis and prognosis in invasive breast carcinoma. Cancer Res. 1996; 56:4625–4629. [PubMed: 8840975]
26. Leone G, Nuckolls F, Ishida S, Adams M, Sears R, Jakoi L, et al. Identification of a novel E2F3 product suggests a mechanism for determining specificity of repression by Rb proteins. Mol Cell Biol. 2000; 20:3626–3632. [PubMed: 10779352]
27. Lin EY, Nguyen AV, Russell RG, Pollard JW. Colony-stimulating factor 1 promotes progression of mammary tumors to malignancy. J Exp Med. 2001; 193:727–740. [PubMed: 11257139]
28. Lujambio A, Calin G, Villanueva A, Ropero S, Sánchez-Céspedes M, Blanco D, et al. A microRNA DNA methylation signature for human cancer metastasis. Proc Natl Acad Sci U S A. 2008; 105:13556–13561. [PubMed: 18768788]
29. Mootha V, Lindgren C, Eriksson K, Subramanian A, Sihag S, Lehar J, et al. PGC-1alpha-responsive genes involved in oxidative phosphorylation are coordinately downregulated in human diabetes. Nat Genet. 2003; 34:267–273. [PubMed: 12808457]
30. Mundy G, Yoneda T. Bisphosphonates as anticancer drugs. N Engl J Med. 1998; 339:398–400. [PubMed: 9691109]
31. Myers TR, Greenwald I. lin-35 Rb acts in the major hypodermis to oppose ras-mediated vulval induction in C. elegans. Dev Cell. 2005; 8:117–123. [PubMed: 15621535]
32. Nasser MW, Qamri Z, Deol YS, Ravi J, Powell CA, Trikha P, et al. S100A7 enhances mammary tumorigenesis through upregulation of inflammatory pathways. Cancer Res. 2011
33. Nevins JR. The Rb/E2F pathway and cancer. Hum Mol Genet. 2001; 10:699–703. [PubMed: 11257102]
34. O'Shaughnessy J. Extending survival with chemotherapy in metastatic breast cancer. Oncologist. 2005; 10(Suppl 3):20–29. [PubMed: 16368868]
35. Olsson A, Feber A, Edwards S, Te Poele R, Giddings I, Merson S, et al. Role of E2F3 expression in modulating cellular proliferation rate in human bladder and prostate cancer cells. Oncogene. 2007; 26:1028–1037. [PubMed: 16909110]
36. Orimo A, Gupta P, Sgroi D, Arenzana-Seisdedos F, Delaunay T, Naeem R, et al. Stromal fibroblasts present in invasive human breast carcinomas promote tumor growth and angiogenesis through elevated SDF-1/CXCL12 secretion. Cell. 2005; 121:335–348. [PubMed: 15882617]
37. Pawitan Y, Bjöhle J, Amler L, Borg AL, Egyhazi S, Hall P, et al. Gene expression profiling spares early breast cancer patients from adjuvant therapy: derived and validated in two population-based cohorts. Breast Cancer Res. 2005; 7:R953–964. [PubMed: 16280042]
38. Reynolds LE, Watson AR, Baker M, Jones TA, D'Amico G, Robinson SD, et al. Tumour angiogenesis is reduced in the Tc1 mouse model of Down's syndrome. Nature. 2010; 465:813–817. [PubMed: 20535211]
39. Sangaletti S, Stoppacciaro A, Guiducci C, Torrisi MR, Colombo MP. Leukocyte, rather than tumor-produced SPARC, determines stroma and collagen type IV deposition in mammary carcinoma. J Exp Med. 2003; 198:1475–1485. [PubMed: 14610043]
40. Stetler-Stevenson WG, Aznavoorian S, Liotta LA. Tumor cell interactions with the extracellular matrix during invasion and metastasis. Annu Rev Cell Biol. 1993; 9:541–573. [PubMed: 8280471]
41. Talmadge J, Donkor M, Scholar E. Inflammatory cell infiltration of tumors: Jekyll or Hyde. Cancer Metastasis Rev. 2007; 26:373–400. [PubMed: 17717638]
42. Trikha P, Sharma N, Opavsky R, Reyes A, Pena C, Ostrowski MC, et al. E2f1-3 are critical for myeloid development. J Biol Chem. 2011; 286:4783–4795. [PubMed: 21115501]
43. van de Vijver MJ, He YD, van't Veer LJ, Dai H, Hart AA, Voskuil DW, et al. A gene-expression signature as a predictor of survival in breast cancer. N Engl J Med. 2002; 347:1999–2009. [PubMed: 12490681]
44. Van Nguyen A, Pollard JW. Colony stimulating factor-1 is required to recruit macrophages into the mammary gland to facilitate mammary ductal outgrowth. Dev Biol. 2002; 247:11–25. [PubMed: 12074549]
45. Wang Y, Klijn JG, Zhang Y, Sieuwerts AM, Look MP, Yang F, et al. Gene-expression profiles to predict distant metastasis of lymph-node-negative primary breast cancer. Lancet. 2005; 365:671–679. [PubMed: 15721472]

46. Wu L, de Bruin A, Wang H, Simmons T, Cleghorn W, Goldenberg LE, et al. Selective roles of E2Fs for ErbB2- and Myc-mediated mammary tumorigenesis. Oncogene. 2013

47. Wyckoff J, Wang W, Lin E, Wang Y, Pixley F, Stanley E, et al. A paracrine loop between tumor cells and macrophages is required for tumor cell migration in mammary tumors. Cancer Res. 2004; 64:7022–7029. [PubMed: 15466195]

48. Yue W, Sun Q, Landreneau R, Wu C, Siegfried JM, Yu J, et al. Fibulin-5 suppresses lung cancer invasion by inhibiting matrix metalloproteinase-7 expression. Cancer Res. 2009; 69:6339–6346. [PubMed: 19584278]

49. Ziebold U, Lee EY, Bronson RT, Lees JA. E2F3 loss has opposing effects on different pRB-deficient tumors, resulting in suppression of pituitary tumors but metastasis of medullary thyroid carcinomas. Mol Cell Biol. 2003; 23:6542–6552. [PubMed: 12944480]

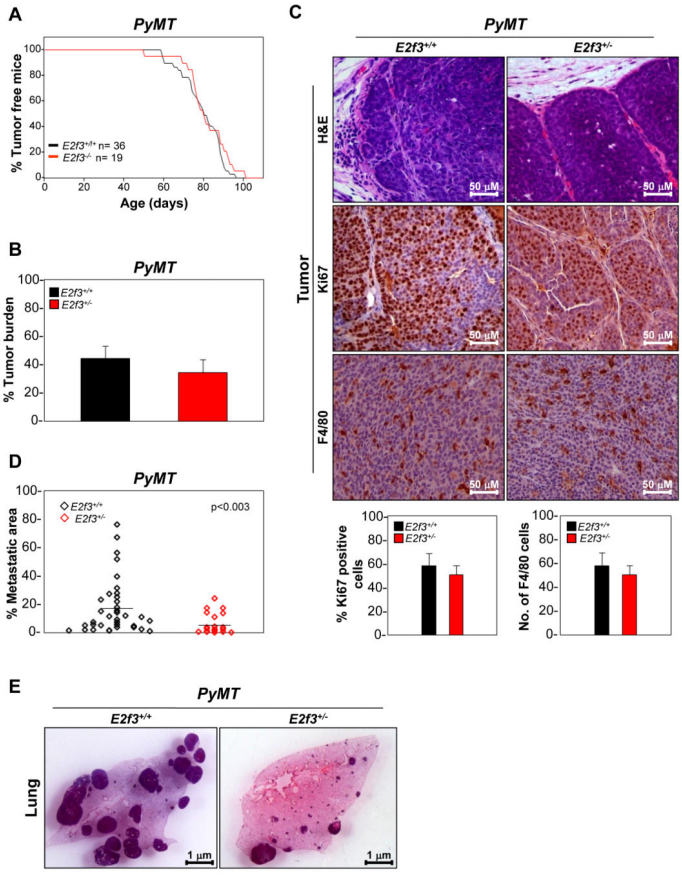

Figure 1. Loss of one *E2f3* allele results in reduction of lung metastasis

(A) Kaplan–Meier tumor-free curves (time from birth to tumor onset) of *MMTV-PyMT; E2f3*$^{+/+}$ (black line) and *MMTV-PyMT; E2f3*$^{+/-}$ (red line) mice. The number of mice in each cohort is indicated by n.

(B) Bar graphs showing tumor burden of mice described above. The mammary tumors were harvested from mice at termination of the study at 110 days. Percent tumor burden was calculated as described in methods. No significant difference was observed between *MMTV-PyMT; E2f3*$^{+/+}$ (black bar) and *MMTV-PyMT; E2f3*$^{+/-}$ (red bar). Values represent mean ± SD.

(C) Paraffin sections of mammary tumors from 110-day old mice *MMTV-PyMT;E2f3*$^{+/+}$ (left) and *MMTV-PyMT;E2f3*$^{+/-}$ (right) mice were stained with H&E (top panel), Ki67 (middle panel) or F4/80 (bottom panel). The Ki67 or F4/80 positive cells were quantified from section as described above.

(D) Analysis of the metastatic area in lungs isolated from *MMTV-PyMT; E2f3*$^{+/+}$ (black diamonds) and *MMTV-PyMT; E2f3*$^{+/-}$ (red diamonds). Percentage metastatic area was calculated from the H&E section from all five lobes of lungs. The data represents the mean of each genotype indicated by horizontal line. Significant difference was observed between the two groups ($p<0.003$).

(E) Representative picture of H&E stained lung showing metastatic lesion in mice from *MMTV-PyMT; E2f3*$^{+/+}$ (left) and *MMTV-PyMT; E2f3*$^{+/-}$ (right).

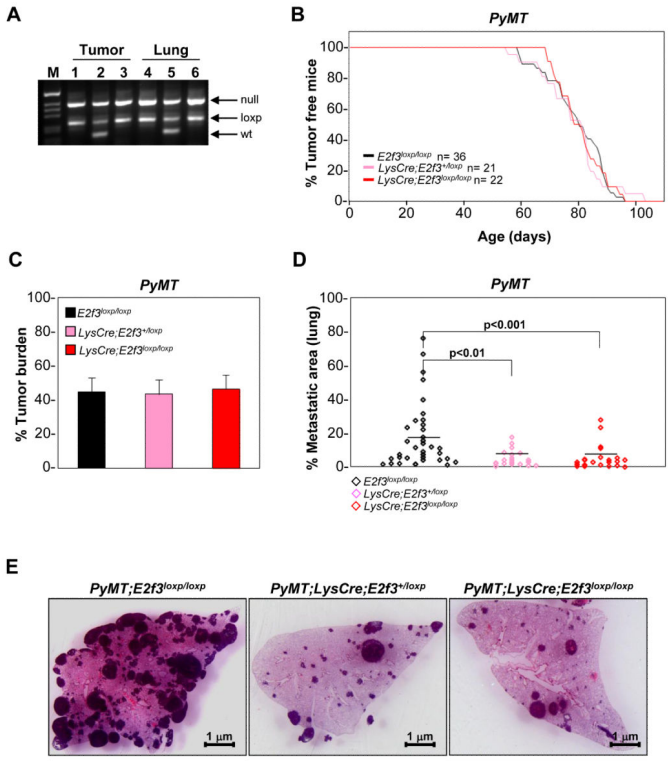

Figure 2. Deletion of *E2f3* in macrophages leads to attenuation of lung metastasis

(A) *E2f3* genotyping on genomic DNA isolated from TAMs of *MMTV-PyMT; LysCre; E2f3$^{loxp/loxp}$* (lanes 1, 3, 4 and 6) and *MMTV-PyMT; LysCre; E2f3$^{+/loxp}$* (lanes 2 and 5) mice.

(B) Kaplan–Meier tumor-free curves (time from birth to tumor onset) of *MMTV-PyMT; E2f3$^{loxp/loxp}$* (black line), *MMTV-PyMT;LysCre;E2f3$^{+/loxp}$* (pink line) and *MMTV-PyMT; LysCre;E2f3$^{loxp/loxp}$* (red line) cohorts. The number of mice in each cohort is indicated by n.

(C) Bar graphs showing tumor burden of mice. The tumors were harvested from mice at termination of the study at 110 days. Percent tumor burden was calculated as described in methods. *MMTV-PyMT; E2f3$^{loxp/loxp}$* (black bar), *MMTV-PyMT; LysCre; E2f3$^{+/loxp}$* (pink bar) and *MMTV-PyMT; LysCre; E2f3$^{loxp/loxp}$* (red bar). Values represent mean ± SD.

(D) Analysis of metastasis in lungs isolated from *MMTV-PyMT; E2f3$^{loxp/loxp}$* (black diamonds), *MMTV-PyMT; LysCre; E2f3$^{+/loxp}$* (pink diamonds) and *MMTV-PyMT; LysCre; E2f3$^{loxp/loxp}$* (red diamonds). Percentage metastatic area was calculated from the H&E section from all five lobes of lungs. The data represents the mean of each genotype indicated by horizontal line.

(E) Representative picture of H&E stained lung showing metastatic lesion in mice from *MMTV-PyMT; E2f3$^{loxp/loxp}$*, *MMTV-PyMT; LysCre; E2f3$^{+/loxp}$* and *MMTV-PyMT; LysCre; E2f3$^{loxp/loxp}$*.

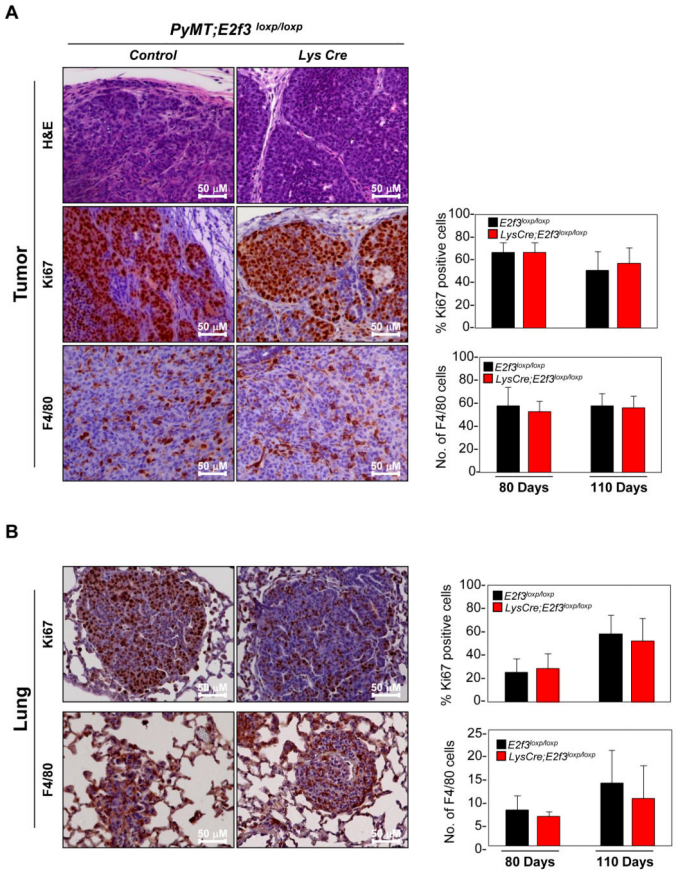

Figure 3. *E2f3* is not required for macrophages proliferation

H&E and immuno-histochemistry of tumors isolated from 110- or 80- day old *MMTV-PyMT;E2f3*$^{loxp/loxp}$ (*control*) and *MMTV-PyMT; LysCre;E2f3*$^{loxp/loxp}$ mice. (A) Mammary tumors and (B) Lungs. The paraffin sections were stained using Ki67- and F4/80- antibodies. Quantification of Ki67- and F4/80- positive cells (right panels).

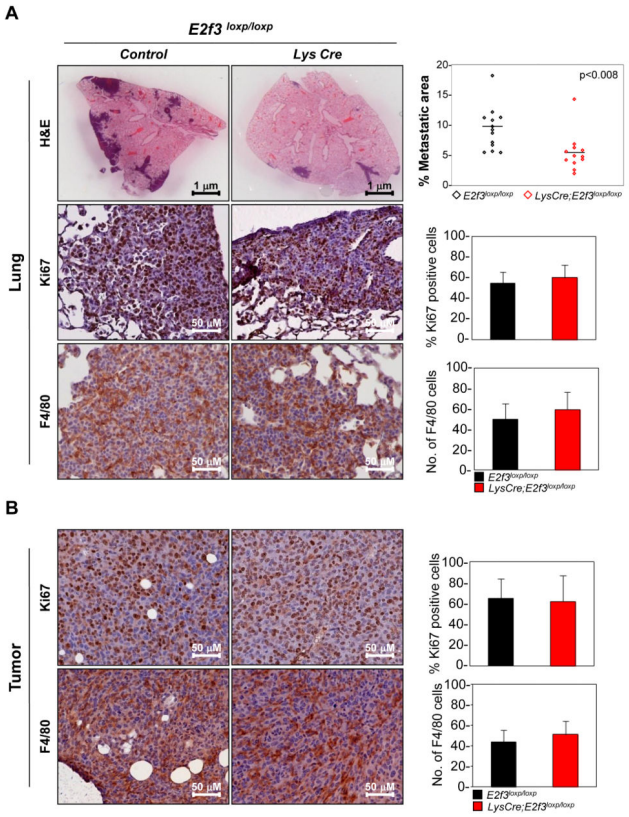

Figure 4. *E2f3* deletion leads to reduction in lung metastasis after orthotopic injection of tumor cells into fat pad

(A) H&E stained section of lung showing metastatic lesions, collected 28 days after injection of MVT-1 cells into mammary fat pad of *LysCre;E2f3*$^{loxp/loxp}$ and *E2f3*$^{loxp/loxp}$ mice. (top panel). A significant reduction in lung metastasis between the two cohorts can be observed ($p<0.008$) (top right panel). Lung section of the indicated genotype stained with Ki67 (middle panel) or macrophage specific F4/80 antibody (bottom panel).

(B) Mammary tumor isolated from the mice described above stained with Ki67 (top panel) and F4/80 (bottom panel). Quantification is depicted in the right panels.

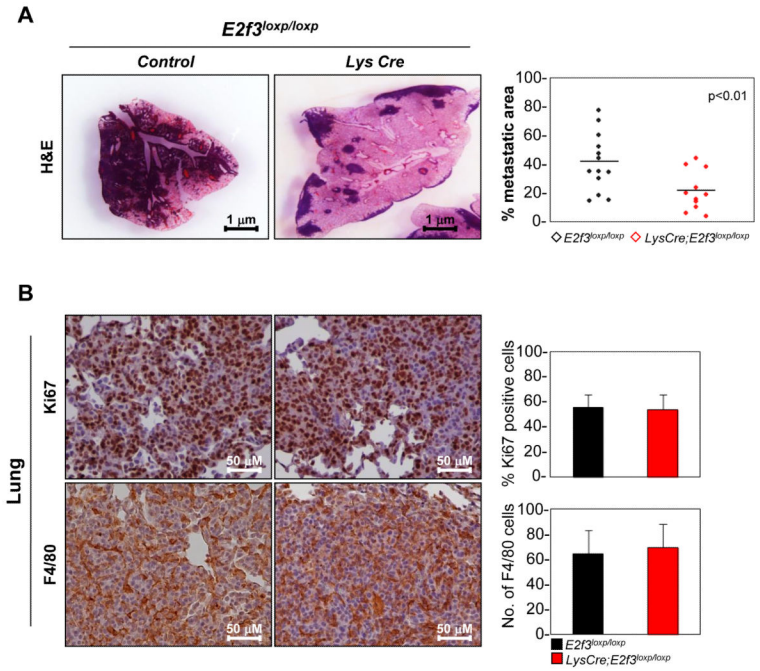

Figure 5. *E2f3* deletion leads to reduction in lung metastasis after tail vein injection of tumor cells

(A) H&E stained section of lung showing metastatic lesions, collected 14 days after the injection of MVT-1 cells into tail vein of *LysCre;E2f3*$^{loxp/loxp}$ and *E2f3*$^{loxp/loxp}$ mice. A significant reduction in lung metastasis between the two cohorts can be observed ($p<0.01$). The data represents the mean of each genotype and is indicated by horizontal line. Quantification of lung metastasis from H&E stained lung sections (top right panel).
(B) Lung sections stained with Ki67 antibody (top panel) or F4/80 antibody (bottom panel). Quantification of Ki67 and F4/80 positive cells. (right panel).

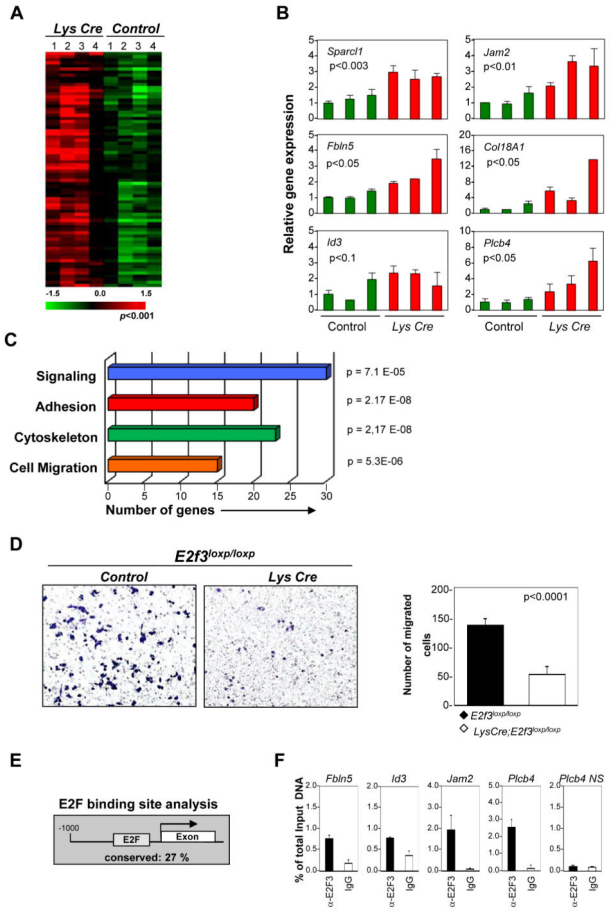

Figure 6. Loss of *E2f3* in TAMs leads to disruption of genes involved in cell adhesion

(A) Heatmap showing hierarchical clustering analysis of genes differentially expressed between *MMTV-PyMT;E2f3*$^{loxp/loxp}$ (*control*) and *MMTV-PyMT; LysCre;E2f3*$^{loxp/loxp}$ mice ($p<0.001$). TAMs isolated from mice of the indicated genotype were used for microarray analysis. Four independent samples were analyzed from each genetic group.

(B) Quantitative real-time PCR to validate the expression of some differentially expressed genes. The value on the *y*-axis represents fold induction.

(C) Gene ontology performed on the differentially expressed genes as determined by the Ingenuity Pathway Analysis ($p<0.001$).

(D) Representative image showing the rate of migration of MVT-1 cells in response to conditioned media obtained from TAMs of indicated genotypes (left panel). Quantification of number of migrated MVT-1 cells (right panel). Values represent mean ± SD

(E) The figure depicts percentage of E2F sites conserved between the human and mouse promoter.

(F) ChIP assay showing E2F3 recruitment on promoters of genes in wild type TAMs. No E2F3 loading is observed on promoters devoid of E2f binding site ‘no site (NS)’.

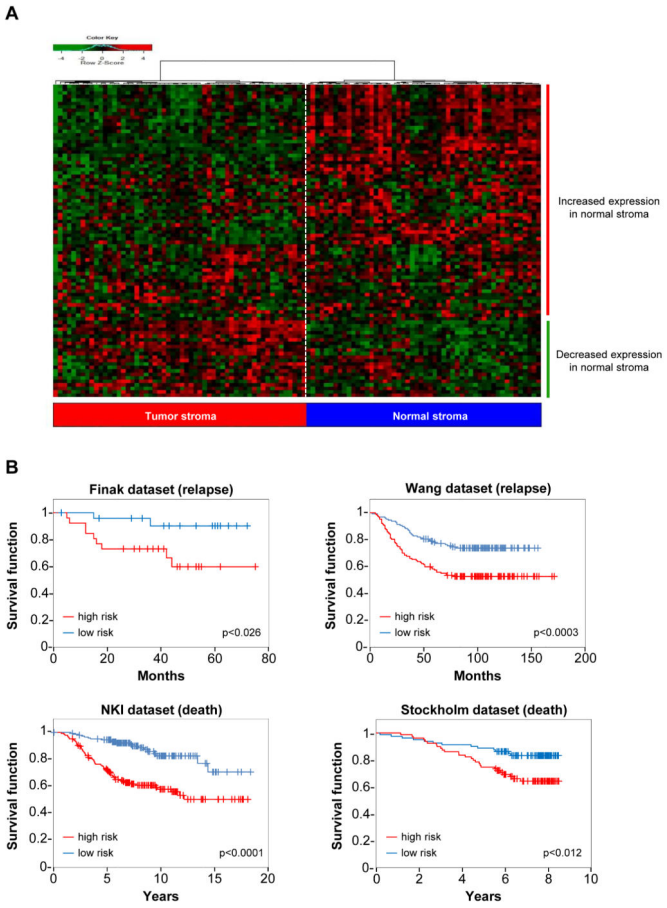

Figure 7. *E2f3* TAM gene signature predicts survival in human breast cancer patient datasets

(A) Heat map displaying the human orthologs corresponding to differentially expressed genes from mouse *E2f3* TAM list using Finak dataset. The dendogram obtained from a hierarchical clustering with Euclidean distances is shown on top of the heat map. Red and green regions in the heat map indicate genes that are up-regulated or down-regulated with respect to the median gene expression over the patients.

(B) Kaplan-Meier plots predicting overall survival using Finak, Wang, NKI and Stockholm breast cancer datasets.